

## Supporting Information

### **Efficient Faradaic Supercapacitor Energy Storage using Redox-Active Pyrene- and Benzodithiophene-4,8-dione-Tethered Conjugated Microporous Polymers**

Taher A. Gaber,<sup>1†</sup> Lamiaa Reda Ahmed<sup>1,2†</sup> and Ahmed F. M. EL-Mahdy<sup>1,3\*</sup>

[1] Department of Materials and Optoelectronic Science, National Sun Yat-Sen University, Kaohsiung 80424, Taiwan

[2] Institute of Medical Science and Technology, National Sun Yat-Sen University, Kaohsiung, 80424, Taiwan.

[3] Chemistry Department, Faculty of Science, Assiut University, Assiut 71516, Egypt

† These two authors contributed equally.

Corresponding authors:

Ahmed F. M. EL-Mahdy, +886-986-404-402, E-mail:

[ahmedelmahdy@mail.nsysu.edu.tw](mailto:ahmedelmahdy@mail.nsysu.edu.tw)

<b>Section</b>	<b>Content</b>	<b>Page No.</b>
<b>S1</b>	<b>Materials</b>	<b>S3</b>
<b>S2</b>	<b>Characterization</b>	<b>S3</b>
<b>S3</b>	<b>Synthetic Procedures</b>	<b>S4</b>
<b>S4</b>	<b>Spectral Analyses of Monomers</b>	<b>S8</b>
<b>S5</b>	<b>Spectral Analyses of CMPs</b>	<b>S11</b>
<b>S6</b>	<b><sup>13</sup>C CP/MAS NMR spectra of CMPs</b>	<b>S12</b>
<b>S7</b>	<b>X-Ray Photoelectron Spectroscopy Analysis</b>	<b>S12</b>
<b>S8</b>	<b>Thermogravimetric Analysis (TGA) Profiles</b>	<b>S13</b>
<b>S9</b>	<b>Powder X-Ray Diffraction Analysis (XRD) Profiles</b>	<b>S14</b>
<b>S10</b>	<b>BET Parameters</b>	<b>S14</b>
<b>S11</b>	<b>FE-SEM and EDS Mapping of CMPs</b>	<b>S16</b>
<b>S12</b>	<b>Electrochemical Analysis in Three-Electrode System</b>	<b>S16</b>
<b>S13</b>	<b>Electrochemical Analysis in Two-Electrode Symmetric Supercapacitor System</b>	<b>S20</b>
<b>S14</b>	<b>Electrochemical Analysis in Two-Electrode Symmetric Supercapacitor System with organic electrolyte</b>	<b>S21</b>
<b>S15</b>	<b>References</b>	<b>S22</b>

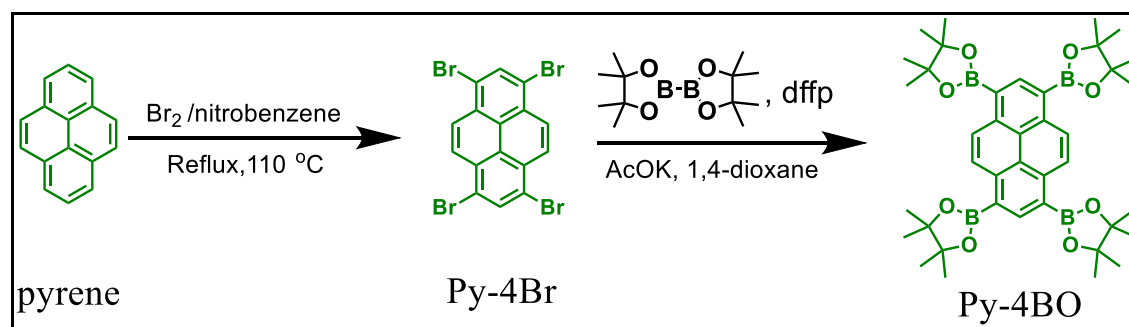
## S1. Materials

Pyrene (98%) and dimethylformamide (DMF) were obtained from Sigma Aldrich. *N*-Butyllithium (*n*-BuLi, 2.5 M in hexane) was ordered from Albemarle. 1,4-phenylenediboronic acid ( $\geq 95\%$ ), tetrakis(triphenylphosphine)palladium (Pd(PPh<sub>3</sub>)<sub>4</sub>), 99%), and *N*-bromosuccinimide (NBS) (99%), were purchased from Acros. Potassium carbonate (K<sub>2</sub>CO<sub>3</sub>) and potassium acetate were supplied from Combi-Blocks.

## S2. Characterization

Fourier-transform infrared spectroscopy (FTIR) spectroscopy was recorded using a Bruker Tensor 27 FTIR spectrophotometer and the conventional KBr plate method; 32 scans were collected at a resolution of 4 cm<sup>-1</sup>. Solid state nuclear magnetic resonance (SSNMR) spectroscopy was recorded using a Bruker Avance 400 NMR spectrometer and a Bruker magic-angle-spinning (MAS) probe, running 32,000 scans. Thermogravimetric analysis (TGA) was performed using a TA Q-50 analyzer under a flow of N<sub>2</sub>. The samples were sealed in a Pt cell and heated from 40 to 700 °C at a heating rate of 20 °C min<sup>-1</sup> under N<sub>2</sub> at a flow rate of 50 mL min<sup>-1</sup>. Nitrogen adsorption-desorption measurements were carried out using a BelSorp max instrument. Before measuring gas adsorption, the as-prepared samples (50 mg) were washed with anhydrous tetrahydrofuran for 24 hours using Soxhlet extraction. The solvent was filtered, and the samples were activated for 10 hours under pressure at 150 °C. The samples were then used for gas adsorption-desorption measurements at 77 K from 0 to 1 atm. Their specific surface areas were calculated using the Brunauer-Emmett-Teller (BET) methodology. The pore distributions were calculated from the sorption data using the quenched solid state density functional theory. Field-emission scanning electron microscopy (FE-SEM) was conducted using a JEOL JSM-7610F scanning electron microscope. Samples were subjected to Pt sputtering for 100 s prior to observation. Transmission electron microscopy (TEM) was performed using a JEOL-2100 scanning electron microscope, operated at 200 kV.

### S3. Synthetic Procedures

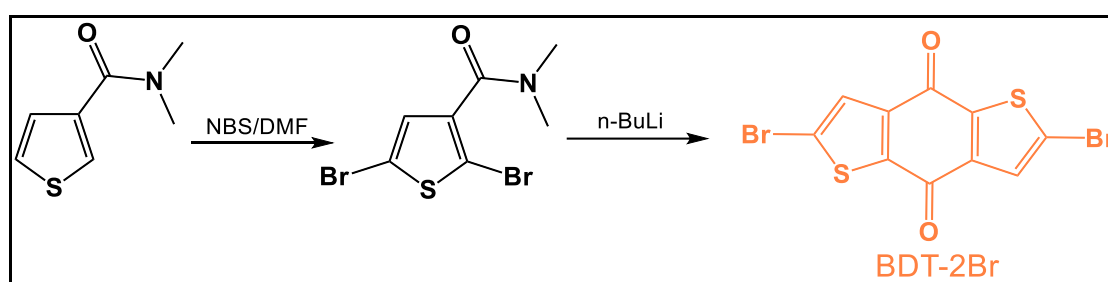


**Scheme S1.** Synthesis of Py-4BO.

**1,3,6,8-tetrabromopyrene (Py-4Br):** was prepared as described in the literature with minor modifications.<sup>S1</sup> A 500 mL round-bottom flask was charged with pyrene (5.0 g, 24 mmol) and nitrobenzene (200 mL) and then bromine (5.6 mL, 109 mmol) was added dropwise through a dropping funnel. The reaction mixture was allowed to reflux at  $120\text{ }^\circ\text{C}$  for 15 hours. After the consumption of bromine, pale yellow crystallites of 1,3,6,8-tetrabromopyrene were separated from the reaction mixture as precipitate. The suspension was filtrate, and the pale-yellow product was washed several times with ethanol and dried under pressure for 12 hours to yield the product in 94%. FTIR:  $1592, 1466, 1450, 1228, 1052, 988, 871, \text{ and } 812\text{ cm}^{-1}$ .

**1,3,6,8-tetrakis(4,4,5,5-tetramethyl-1,3,2-dioxaborolan-2-yl)pyrene (Py-4BO):** A 100 mL round-bottom flask was charged with pyrene-4Br (2.0 g, 3.8 mmol), bis(pinacolato)diboron (5.98 g, 23.56 mmol), [1,1'-Bis(diphenylphosphino)ferrocene] dichloro palladium(II) (241 mg, 0.033 mmol), and potassium acetate (2.33 g, 23.37 mmol). The solids were evacuated under high pressure for 15 minutes. Then, dioxane (40 mL) was added and the reaction mixture allowed to reflux for 48 hours under  $\text{N}_2$ . After the consumption of pyrene-4Br, the reaction mixture was cooled to room-temperature and then poured into ice-water to produce a yellow precipitate. The

precipitate was filtered and washed several times with water and purified using flash column chromatography with THF/hexane as eluent. The isolate solid was finally recrystallized with methanol to give 1,3,6,8-tetrakis(4,4,5,5-tetramethyl-1,3,2-dioxaborolan-2-yl) pyrene (**Py-4BO**) as yellow crystals (1.9 g, 70% yield). FTIR: 2975, 2923, 2853, 1610, 1554, 1336, and 1145  $\text{cm}^{-1}$  (Figure S1).  $^1\text{H}$  NMR (500 MHz,  $\text{CDCl}_3$ )  $\delta$  (ppm): 9.14 (s, 4H) and 8.97 (s, 2H) (Figure S2).  $^{13}\text{C}$  NMR (125 MHz,  $\text{CDCl}_3$ )  $\delta$  (ppm): 138.51, 129.98, 124.40, 84.31, and 25.64 (Figure S3).

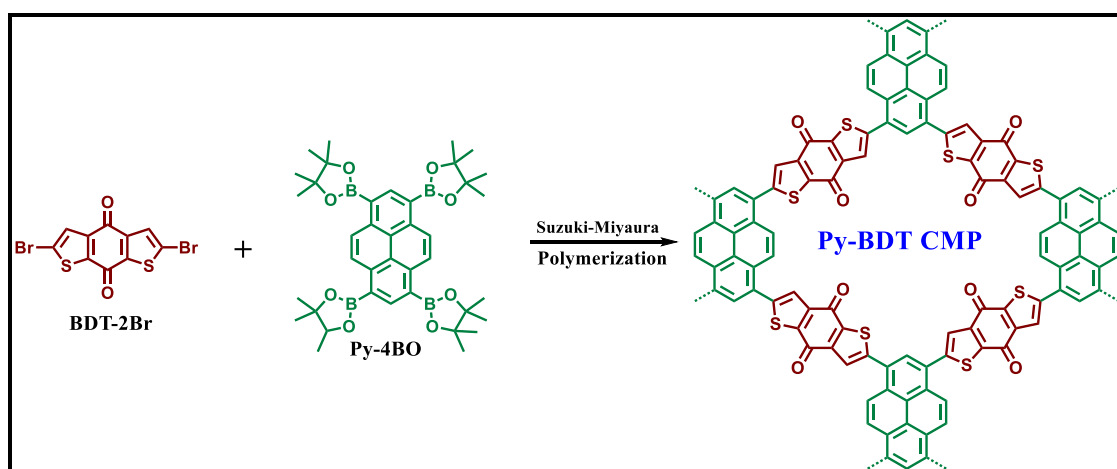


**Scheme S2.** Synthesis of 2,6-dibromobenzo[1,2-b:4,5-b']dithiophene-4,8-dione.

**2,5-dibromo-*N,N*-dimethylthiophene-3-carboxamide:** *N,N*-dimethylthiophene-3-carboxamide (3.0 g, 19.3 mmol) was added to dry dimethylformamide (50 ml) followed by wise dropping of a solution of *N*-bromosuccinimide (8.6 g, 48.25 mmol) dry dimethylformamide (20 ml). The prepared flask was stirred for 4 h at room temperature. The reaction mixture was then added to 600 mL of water, followed by an ethyl acetate extraction. The organic phase was concentrated under reduced pressure. Hexane/ethylacetate (6:1, v/v) was used as the eluent during the silica gel column chromatography of the residue, which produced 2,5-dibromo-*N,N*-dimethylthiophene-3-carboxamide (5.4 g, yield 90 %) as yellow oil.

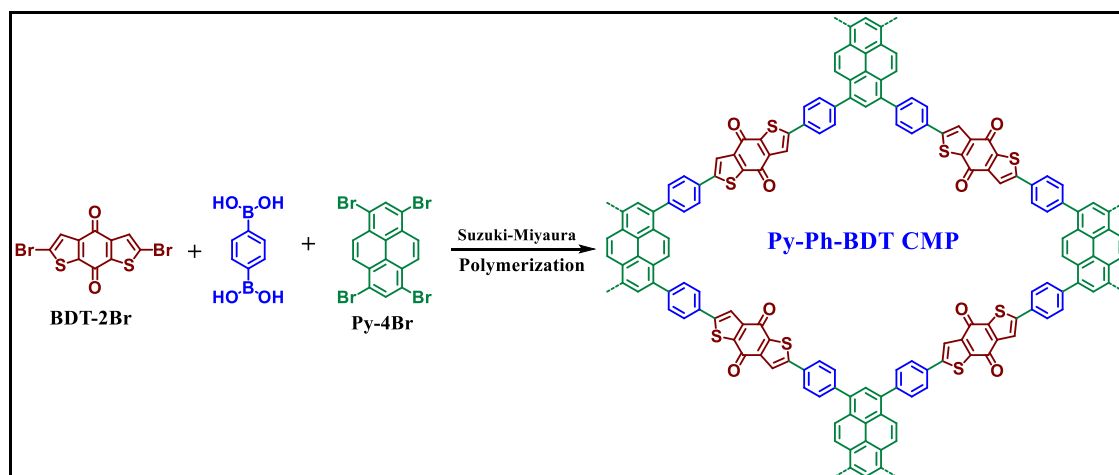
**2,6-dibromobenzo[1,2-b:4,5-b']dithiophene-4,8-dione (BDT-2Br):** In a 250-mL two-neck bottle, A suspension of 2,5-dibromo-*N,N*-dimethylthiophene-3-carboxamide (2.00 g, 6.4 mmol) in dry THF (50 mL) was cooled to  $-78\text{ }^\circ\text{C}$  under a flow of  $\text{N}_2$  and then a solution of *n*-BuLi (2.50 mL, 6.4 mmol, 2.5 M in hexane) was added. The mixture

was stirred at  $-70\text{ }^{\circ}\text{C}$  for 4 h and then warmed to room temperature. The mixture received saturated  $\text{NH}_4\text{Cl}$  aqueous solution (20 mL). After collecting the precipitate, silica gel column chromatography with chloroform as eluent yielded BDT-2Br (1.06 g, yield 44 %) as an orange solid. FTIR: 3096, 1652, 1414, 1382, 1269, 1039, 873, 845, and  $732\text{ cm}^{-1}$  (Figure S4).  $^1\text{H NMR}$  (500 MHz,  $\text{DMSO-d}_6$ )  $\delta$  (ppm): 7.81 (s, 2H) (Figure S5).  $^{13}\text{C NMR}$  (125 MHz,  $\text{DMSO-d}_6$ )  $\delta$  (ppm): 172.84, 145.53, 143.11, 130.16, and 123.68 (Figure S6).



**Scheme S3.** Synthesis of Py-BDT CMP.

BDT-2Br (107.1 mg, 0.28 mmol), Py-4BO (100 mg, 0.14 mmole),  $\text{Pd}(\text{PPh}_3)_4$  (33mg, 0.028 mmol), and  $\text{K}_2\text{CO}_3$  (390 mg, 2.82 mmol) were mixed and placed in a 25 mL Pyrex tube under vacuum for 15 minutes. Then, a DMF/water co-solvent (88:12 v/v%, 12 mL) was added, followed by three freeze/pump/thaw cycles to remove the oxygen. After being flame sealed, the tube was heated for three days at  $130\text{ }^{\circ}\text{C}$ . Once it had dropped to room temperature, the tube was opened, the precipitate was filtered out, and it was washed with methanol. At  $120\text{ }^{\circ}\text{C}$ , the solid was vacuum-dried overnight to produce the Py-BDT CMP as a brown precipitate (yield 80%).



**Scheme S4.** Synthesis of Py-Ph-BDT CMP.

BDT-2Br (146 mg, 0.39 mmol, 2 eq.), Py-4Br (100 mg, 0.193 mmol, 1 eq.), Pd(PPh<sub>3</sub>)<sub>4</sub> (22.3 mg, 0.019 mmol), and Ph-2BO (128 mg, 0.77 mmol, 4 eq.) were mixed and placed in a 50 mL Pyrex tube under vacuum for 15 minutes. Then, DMF (25 mL) and K<sub>2</sub>CO<sub>3</sub> (550 mg in 5 mL water, 3.97 mmol) were added. After being flame sealed, the tube was heated for three days at 130 °C. Once it had dropped to room temperature, the tube was opened, the precipitate was filtered out, and it was washed with methanol. At 120 °C, the solid was vacuum-dried overnight to produce the Py-Ph-BDT CMP as a brown precipitate (yield 81%).

#### S4. Spectral Analyses of Monomers

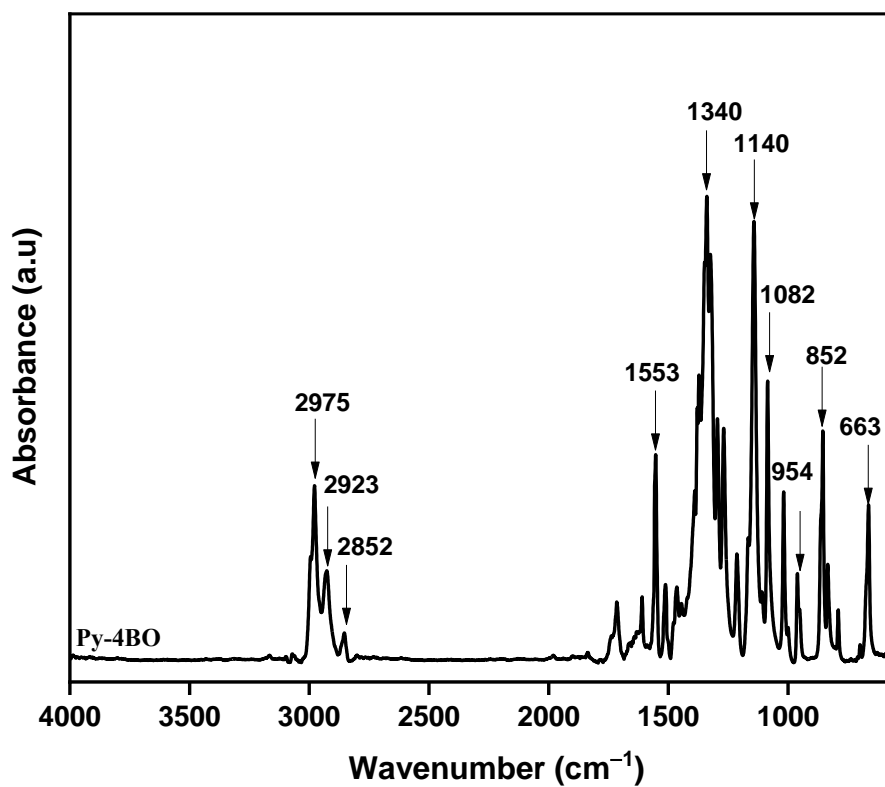


Figure S1. FT-IR spectrum of Py-4BO.

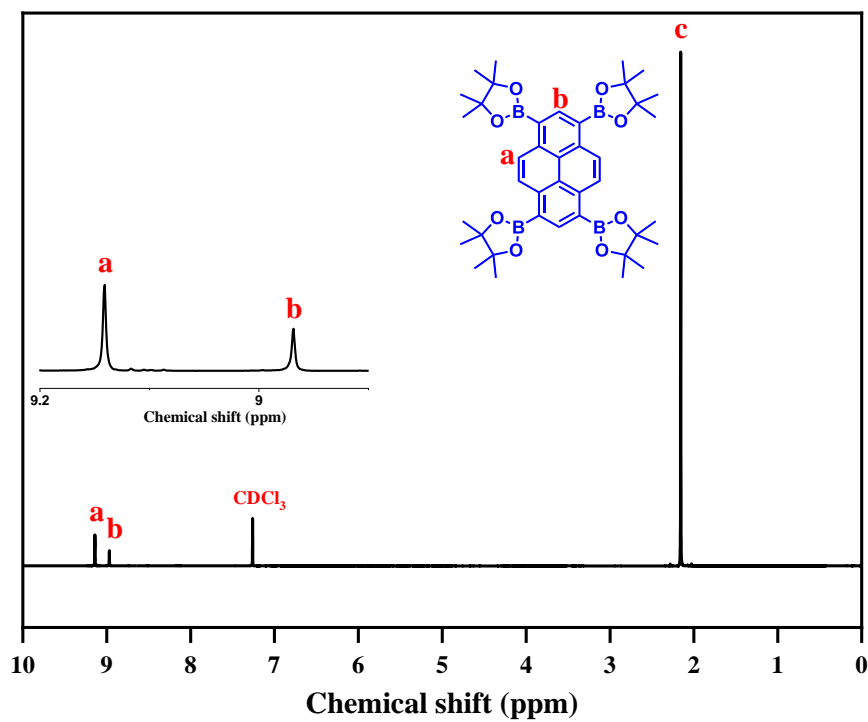
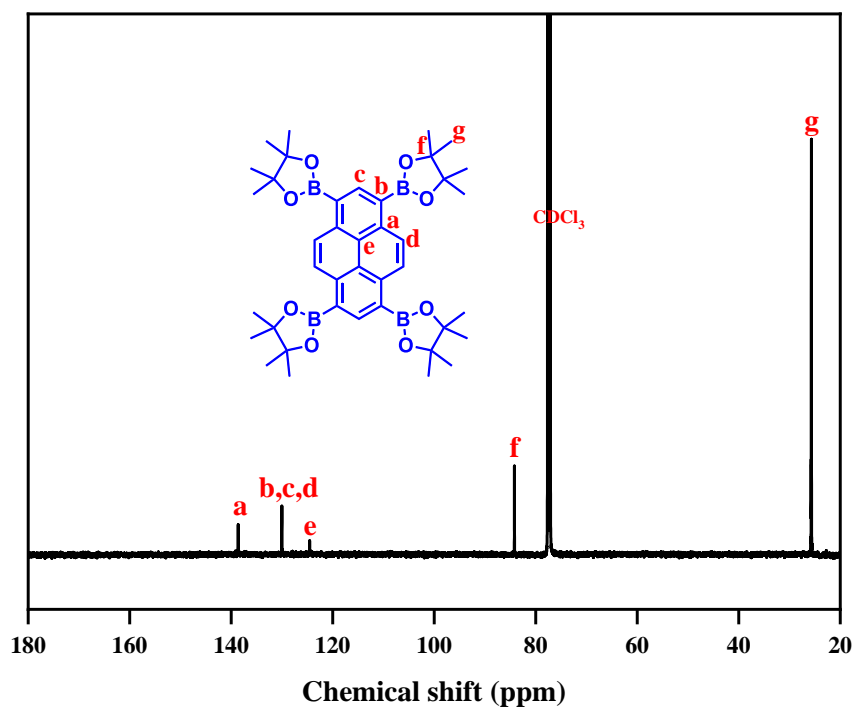
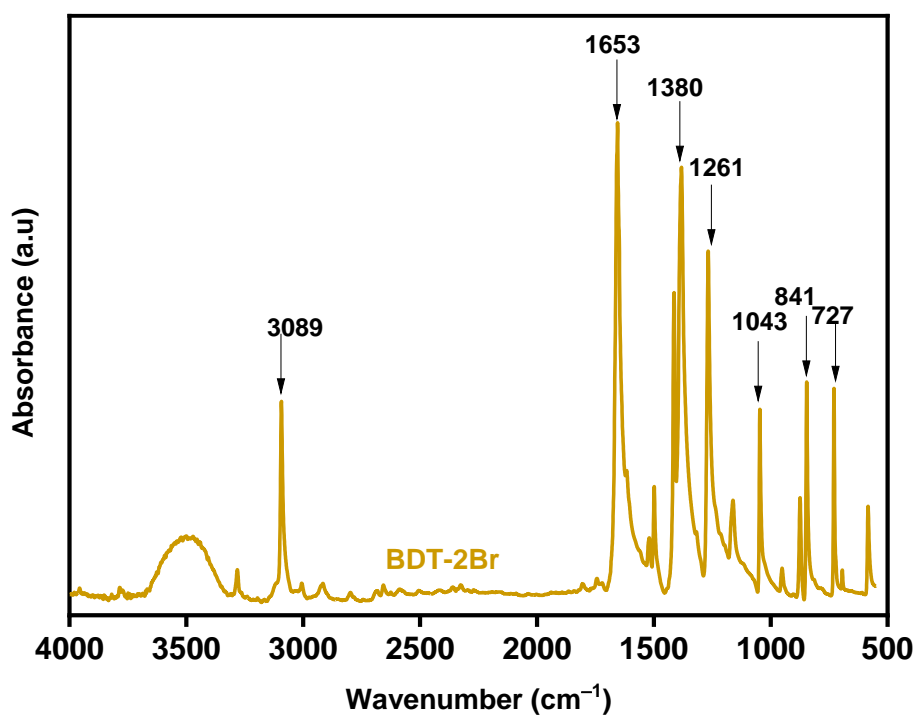


Figure S2.  $^1\text{H-NMR}$  spectrum of Py-4BO.



**Figure S3.**  $^{13}\text{C}$ -NMR spectrum of Py-4BO.



**Figure S4.** FTIR spectrum of BDT-2Br.

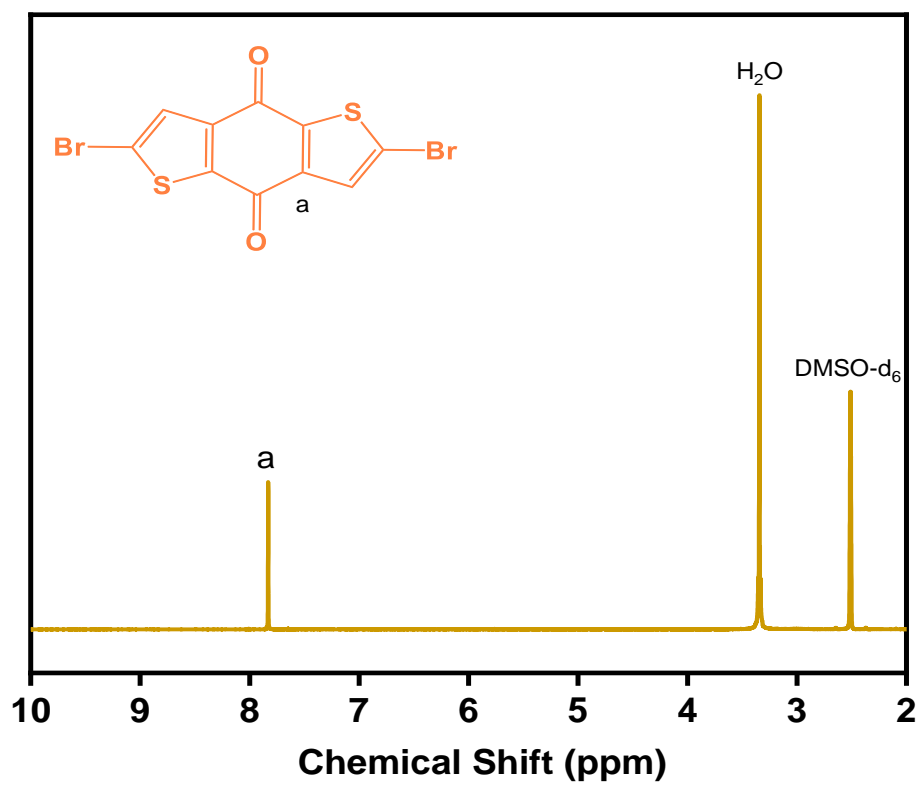


Figure S5.  $^1\text{H}$  NMR spectrum of BDT-2Br.

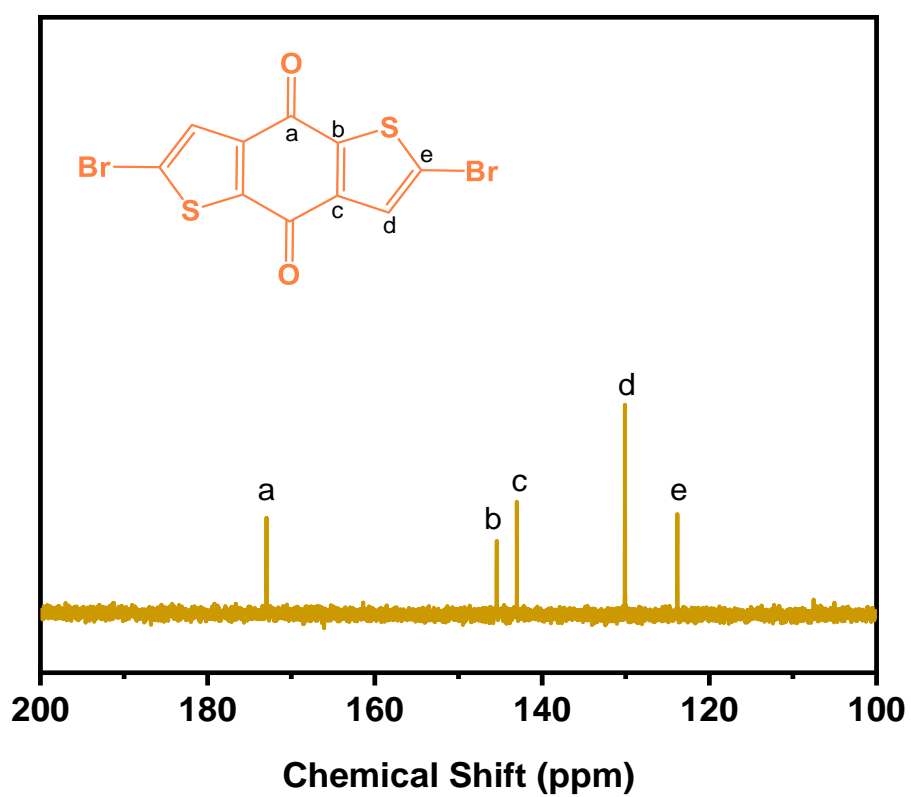


Figure S6.  $^{13}\text{C}$  NMR spectrum of BDT-2Br.

## S5. Spectral Analyses of CMPs

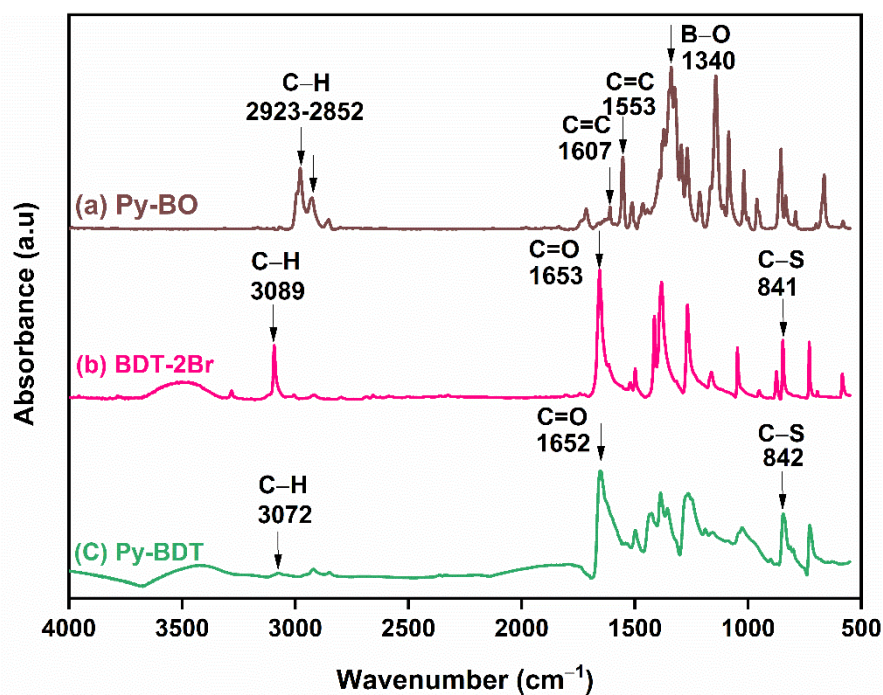


Figure S7. FTIR spectrum of (a) Py-BO, (b) BDT-2Br, and (c) Py-BDT CMP.

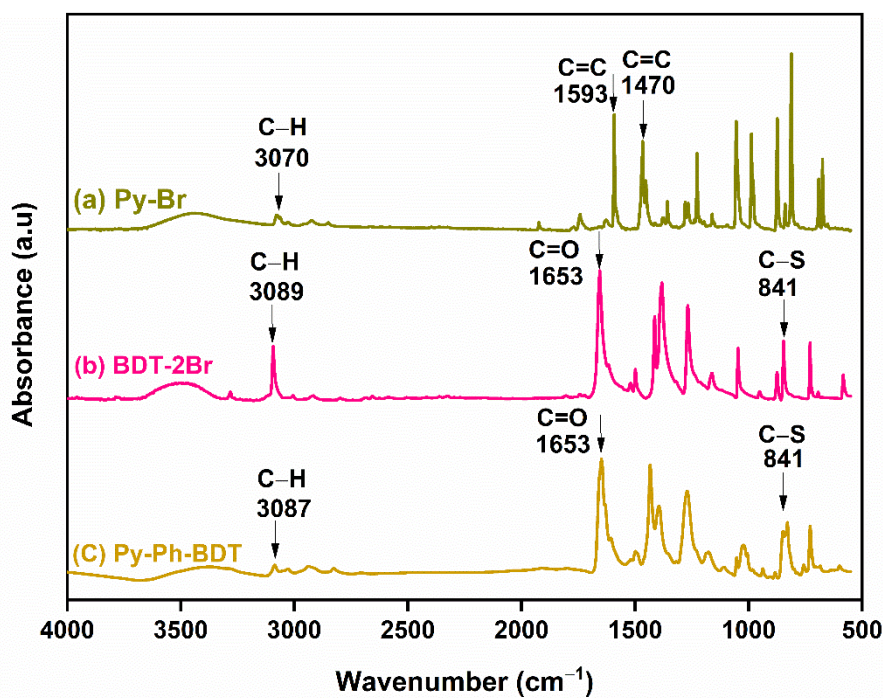


Figure S8. FTIR spectrum of (a) Py-Br, (b) BDT-2Br, and (c) Py-Ph-BDT CMP.

### S6. $^{13}\text{C}$ CP/MAS NMR spectra of CMPs

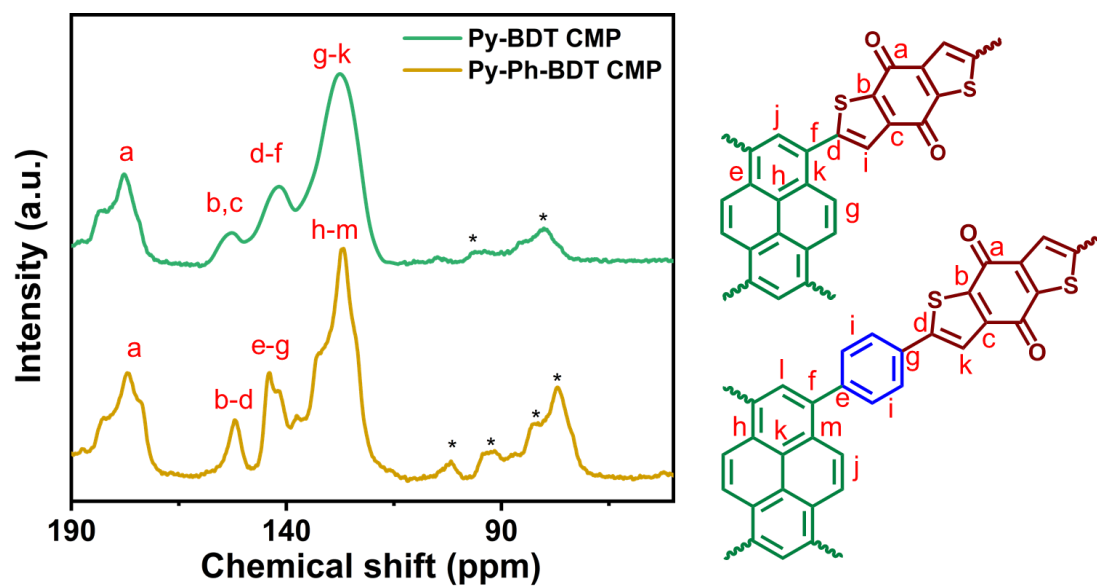


Figure S9.  $^{13}\text{C}$  CP-MAS NMR spectra of the Py-BDT and Py-Ph-BDT CMPs.

### S7. X-Ray Photoelectron Spectroscopy Analysis

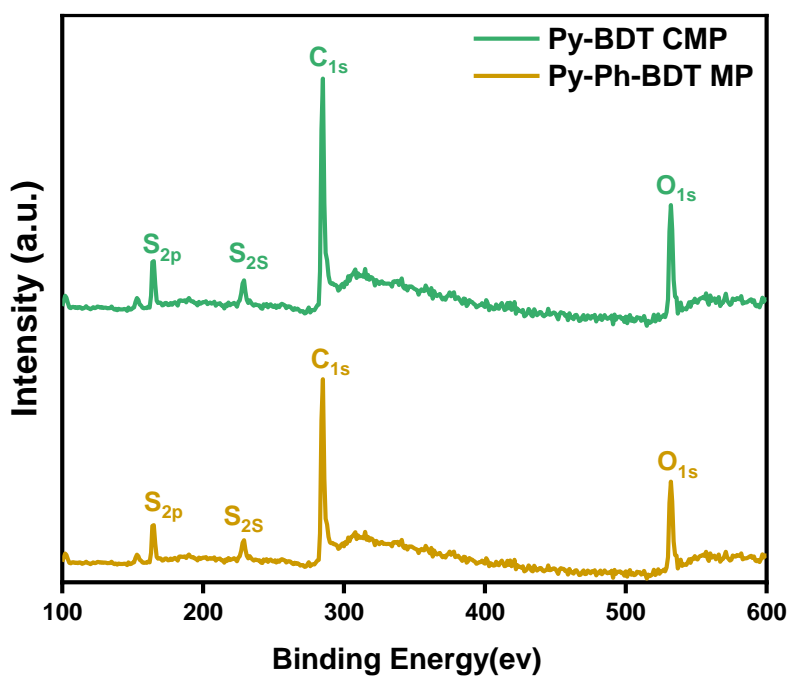
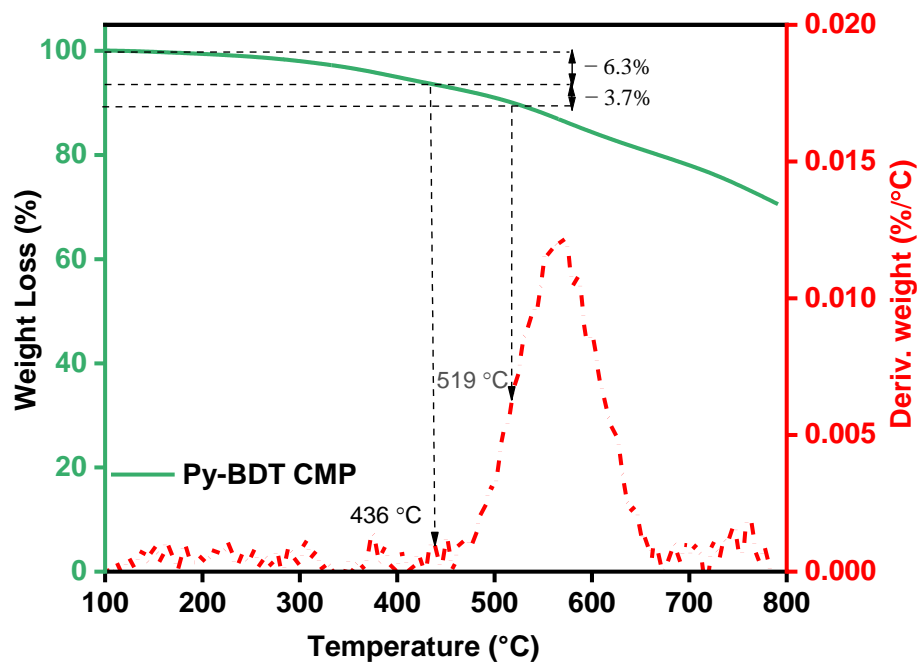


Figure S10. XPS spectra of the Py-BDT and Py-Ph-BDT CMPs.

**Table S1.** XPS fitting positions of the Py-BDT and Py-Ph-BDT CMPs.

Samples		C species			S species		
		C=C	C-S	C=O	S2s	S2p <sub>1/2</sub>	S2p <sub>3/2</sub>
CMPs	Py-BDT	284.40	285.36	287.20	227.67	163.95	165.20
	Py-Ph-BDT	284.33	285.20	286.91	228.73	163.90	164.80

**S8. Thermogravimetric Analysis (TGA) profiles**



**Figure S11.** TGA spectra of Py-BDT CMP.

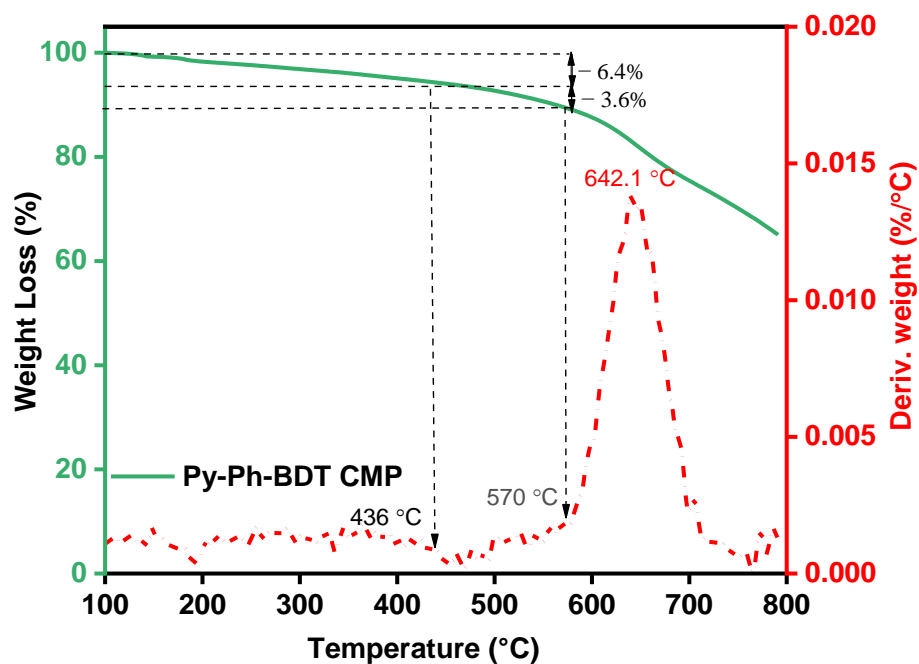


**Figure S12.** TGA spectra of Py-Ph-BDT CMP.

**Table S2.** Values of  $T_{d10\%}$  and Char yield of CMPs.

CMP	$T_{d10}(\text{°C})$	Char yield(%)
Py-BDT	519	70.50
Py-Ph-BDT	570	65.13

### S9. Powder X-Ray Diffraction Analysis (XRD) Profiles

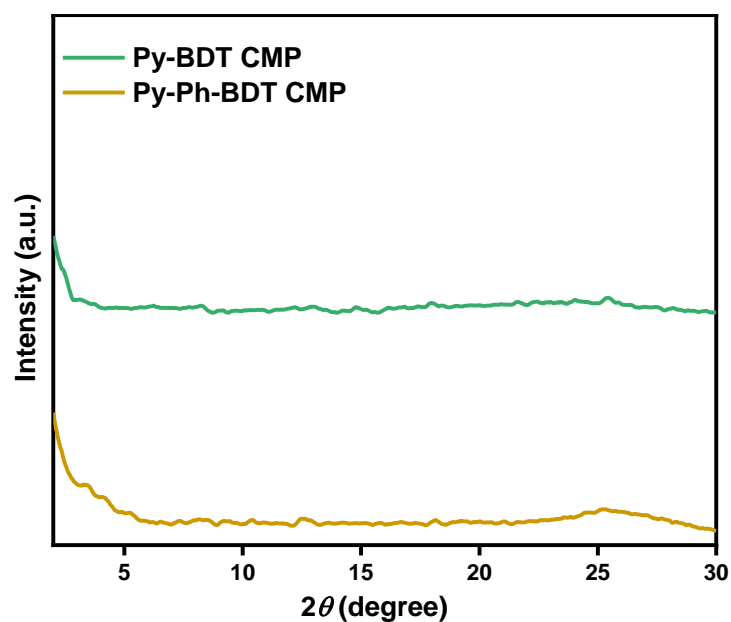


**Figure S13.** PXRD profiles of Py-BDT and Py-Ph-BDT CMPs.

### S10. BET Parameters

**Table S3.** BET parameters of the synthesized CMPs.

CMP	SBET ( $\text{m}^2 \text{g}^{-1}$ )	Pore size (nm)	Pore volume ( $\text{cm}^3 \text{g}^{-1}$ )
Py-BDT	208	1.51-2.63, 3.54-6.38	0.27
Py-Ph-BDT	427	1.52-3.57, 3.66-6.67	0.59

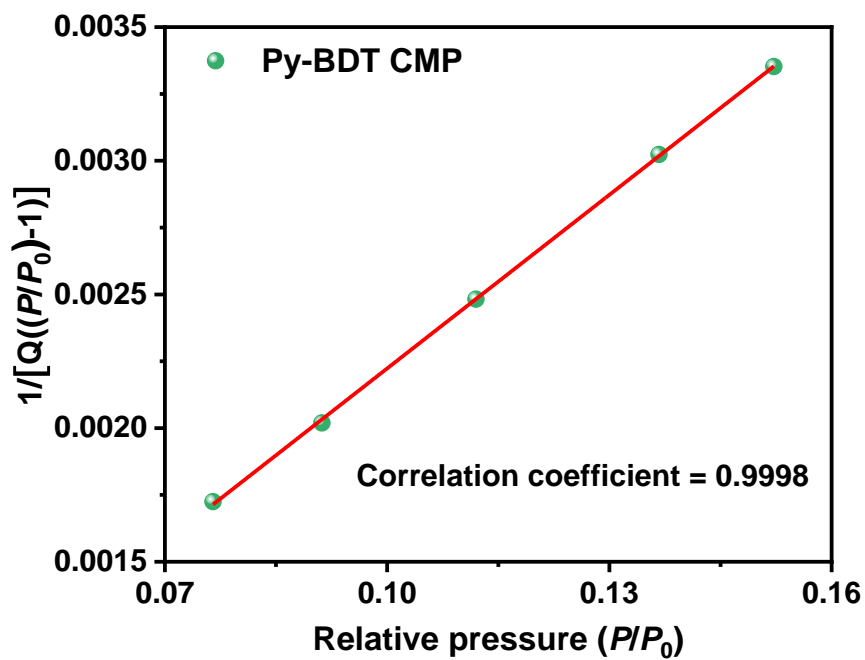


Figure S14. BET linear and linear fitting plots derived from N<sub>2</sub> sorption of Py-BDT CMP.

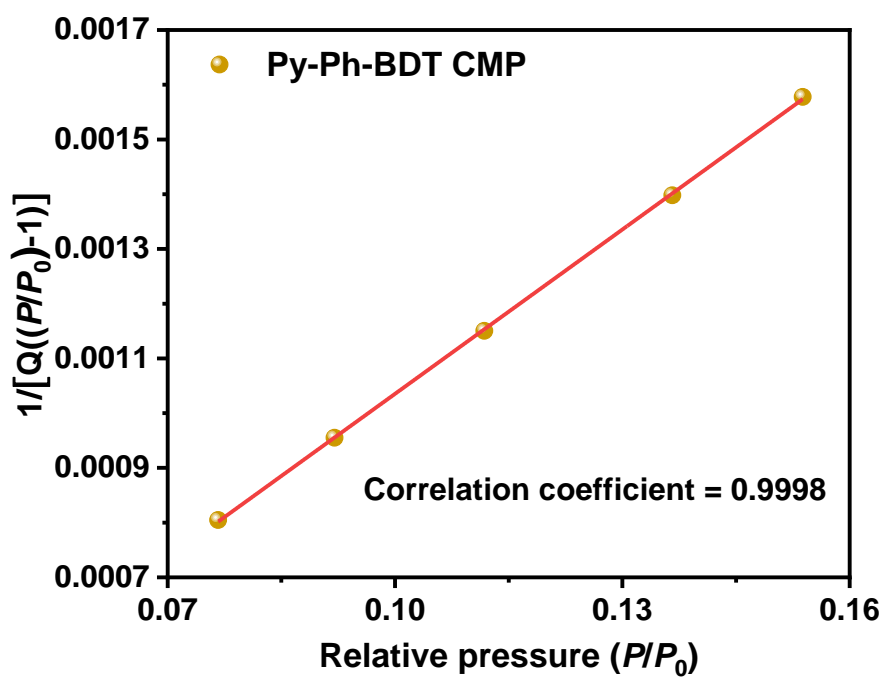
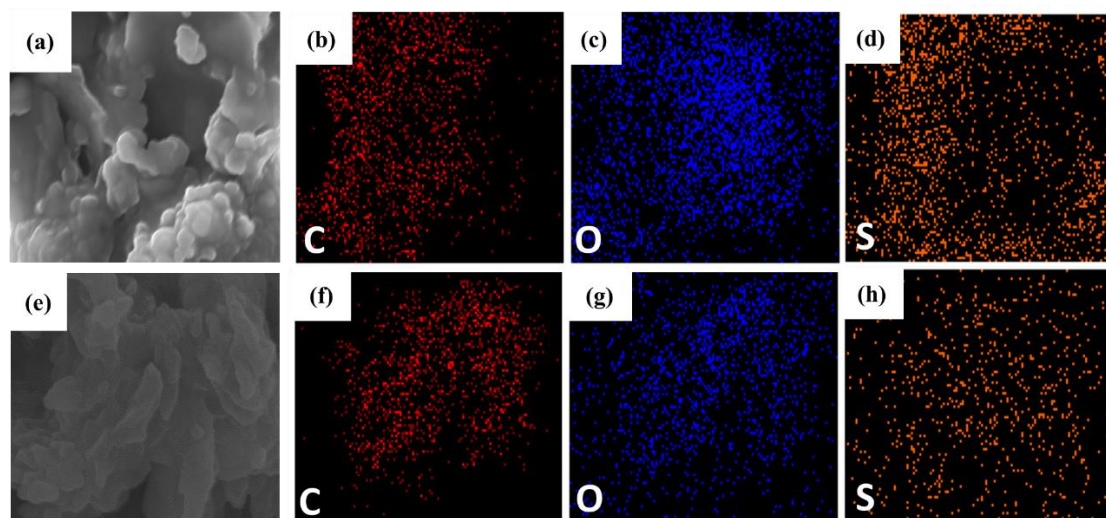


Figure S15. BET linear and linear fitting plots derived from N<sub>2</sub> sorption of Py-Ph-BDT CMP.

## S11. FE-SEM and EDS Mapping of CMPs.



**Figure S16.** FE-SEM photos of (a–d) Py-BDT and (e–h) Py-Ph-BDT CMPs. EDS elemental mapping images of (b–d) Py-BDT and (e–h) Py-Ph-BDT CMPs.

## S12. Electrochemical Analysis in Three-Electrode System

**Working electrode cleaning:** Prior to use, the glassy carbon electrode (GCE) was polished several times with 0.05- $\mu\text{m}$  alumina powder, washed with EtOH after each polishing step, cleaned via sonication (5 min) in a water bath, washed with EtOH, and then dried in air.

**Electrochemical Characterization:** The electrochemical experiments were measured in a three-electrode cell using an Autolab potentiostat (PGSTAT204) in aqueous electrolyte 1 M KOH. The glassy carbon electrode (GCE) was used as the working electrode (diameter: 5.61 mm; 0.2475  $\text{cm}^2$ ). A platinum wire was used as the counter electrode; Hg/HgO (RE-61AP, BAS) was used as the reference electrode. All reported potentials refer to the Hg/HgO potential. The GCE was modified with CMP slurries as described elsewhere with some modifications.<sup>S2-S4</sup> The slurries were prepared by dispersing CMP (80 wt. %), carbon black (15 wt. %), and Nafion (5 wt. %) in 2 mL of ethanol and sonicated for one hour. A portion of this slurry (10  $\mu\text{L}$ ) was pipetted onto

the tip of the electrode which was then dried in air for 30 minutes before use. The electrochemical performance was studied using cyclic voltammetry (CV) at different sweep rates from 5 to 200 mV s<sup>-1</sup>, galvanostatic charge–discharge (GCD) in the potential range from 0.18 to –0.92 V vs. Hg/HgO at different current densities from 2 to 20 A g<sup>-1</sup> in a 1 M KOH aqueous electrolyte solution.

The specific capacitance was calculated from galvanostatic charge–discharge experiments using the following equation:<sup>S4,S5</sup>

$$C_s = (I\Delta t)/(m\Delta V) \quad (S1)$$

Where  $C_s$  (F/g) is specific capacitance of the supercapacitor,  $I$  (A) is the discharge current,  $\Delta V$  (V) is the potential window,  $\Delta t$  (s) is the discharge time, and  $m$  (g) is the mass of the electrode sample being coated on the glassy carbon.

The energy density ( $E$ , Wh/kg), and the power density ( $P$ , W/kg) were calculated using the following equations:<sup>S5</sup>

$$E = 1000C(\Delta V)^2/(2*3600) \quad (S2)$$

$$P = E/(t/3600) \quad (S3)$$

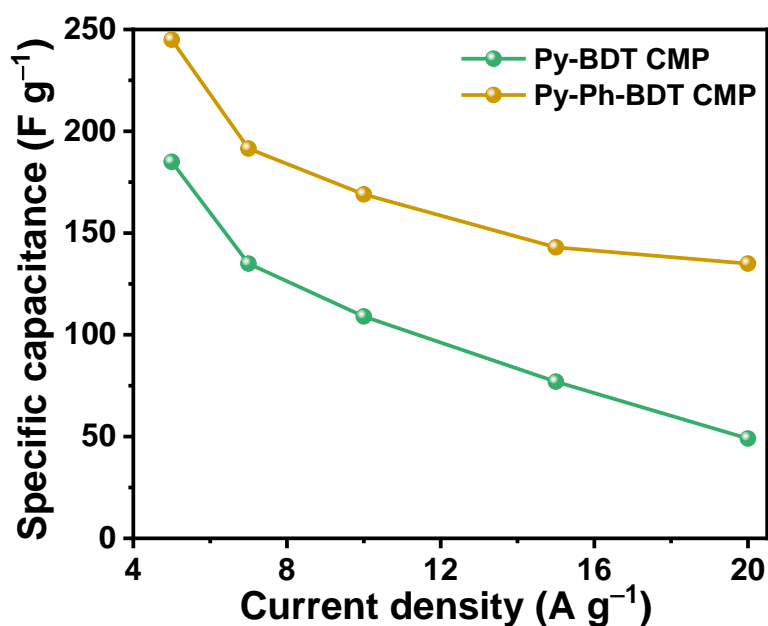


**Figure S17.** Calculated specific capacitances of the Py-BDT and Py-Ph-BDT CMPs, performed at current densities from 5 to 20 A g<sup>-1</sup>.

**Table S4.** Comparison between the specific surface area/specific capacitance Py-BDT and Py-Ph-BDT CMPs with those of previously reported conjugated porous polymers for supercapacitor application.

Polymers	S <sub>BET</sub> (m <sup>2</sup> g <sup>-1</sup> )	Capacitance	Ref.
Py-BDT	208	636 F g <sup>-1</sup> at 0.5 A g <sup>-1</sup>	<b>This work</b>
Py-Ph-BDT	427	712 F g <sup>-1</sup> at 0.5 A g <sup>-1</sup>	<b>This work</b>
MWCNT@SACMP-3	514	594 F g <sup>-1</sup> at 1.0 A g <sup>-1</sup>	<i>ACS Appl. Energy Mater.</i> 2022, <b>5</b> , 3706–3714
4KT-Tp COF	672	583 F g <sup>-1</sup> at 0.2 A g <sup>-1</sup>	<i>CCS Chemistry</i> , 2021, <b>3</b> , 696–706
PAQTA	331	576 F g <sup>-1</sup> at 1.0 A g <sup>-1</sup>	<i>Adv. Mater.</i> 2018, <b>30</b> , 1705710
Fc-CMPs/rGO	800.1	470 F g <sup>-1</sup> at 0.5 A g <sup>-1</sup>	<i>J. Mater. Chem. A</i> , 2018, <b>6</b> , 18827–18832
TCNQ	4000	383 F g <sup>-1</sup> at 0.2 A g <sup>-1</sup>	<i>Angew. Chem. Int. Ed. Engl.</i> 2018, <b>57</b> , 7992–7996
TPDA-1	545	348 F g <sup>-1</sup> at 0.5 A g <sup>-1</sup>	<i>ACS Sustain. Chem. Eng.</i> 2017, <b>6</b> , 202–209
PDC-MA	748.2	335 F g <sup>-1</sup> at 1.0 A g <sup>-1</sup>	<i>ACS Appl. Mater. Interfaces</i> 2019, <b>11</b> , 26355–26363
COF/rGO	246	269 F g <sup>-1</sup> at 0.5 A g <sup>-1</sup>	<i>Nature Commun.</i> 2020, <b>11</b> , 4712.
CAP-2	594	233 F g <sup>-1</sup> at 1.0 A g <sup>-1</sup>	<i>ACS Nano.</i> 2018, <b>12</b> , 852–860
GH-CMP	219	206 F g <sup>-1</sup> at 0.5 A g <sup>-1</sup>	<i>ChemElectroChem</i> 2019, <b>6</b> , 5946–5950
TAT-CMP-2	106	183 F g <sup>-1</sup> at 1.0 A g <sup>-1</sup>	<i>Chem Sci.</i> 2017, <b>8</b> , 2959–2965.
CMP-BT (180 KHz)	372	251 F g <sup>-1</sup> at 10 mV s <sup>-1</sup>	<i>ACS Appl. Mater. Interfaces</i> 2021, <b>13</b> , 61598–61609
CMP-TPA (180 KHz)	542	91.4 F g <sup>-1</sup> at 10 mV s <sup>-1</sup>	<i>ACS Appl. Mater. Interfaces</i> 2021, <b>13</b> , 61598–61609

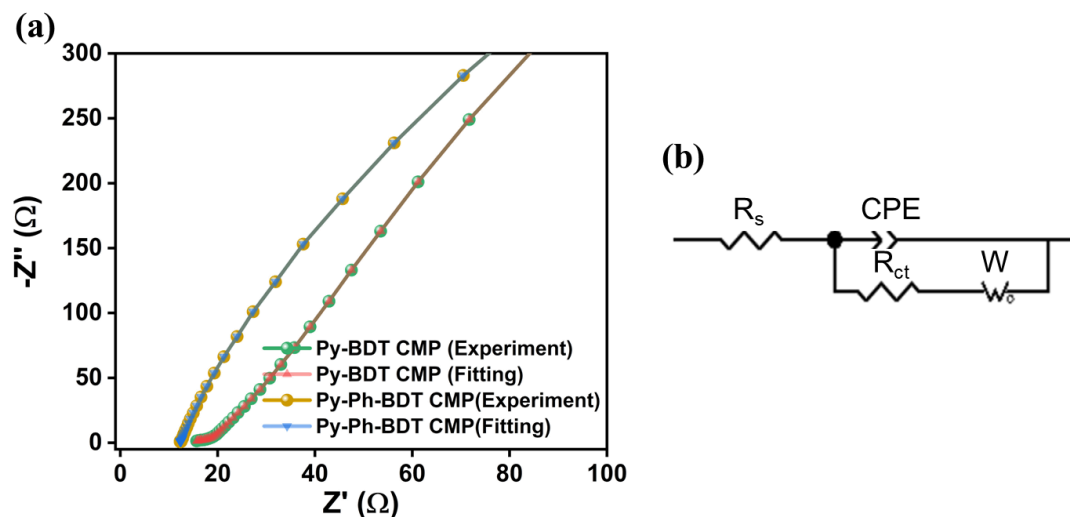


**Figure S18.** (a) The fitted Nyquist plots using (b) the equivalent circuit of Py-BDT and Py-Ph-BDT CMPs.

**Table S5.** The fitting values of Nyquist plots of of Py-BDT and Py-Ph-BDT CMPs.

CMP	$R_s$ ( $\Omega$ )	$R_{ct}$ ( $\Omega$ )
Py-BDT	17.29	10586
Py-Ph-BDT	12.09	6211

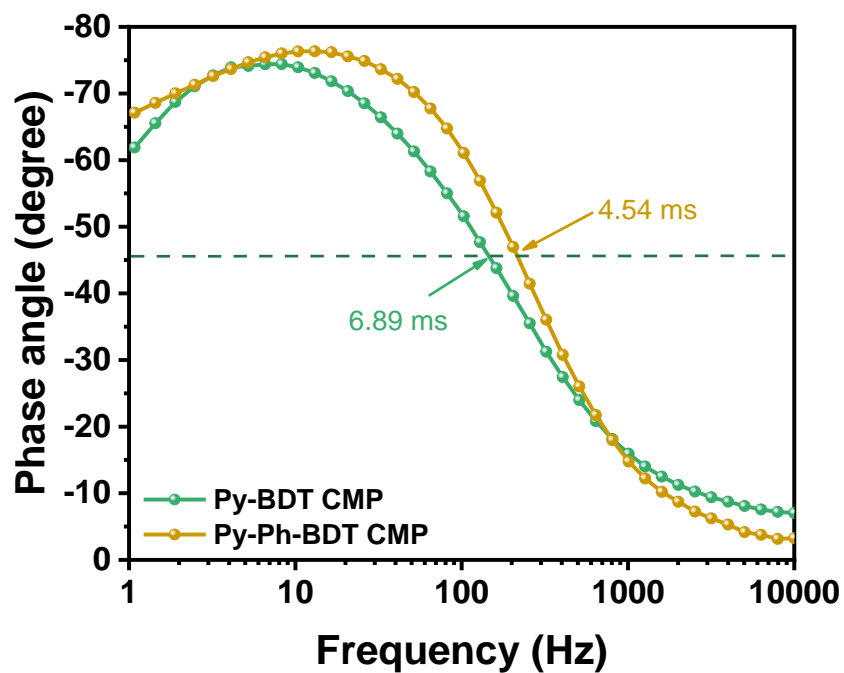


**Figure S19.** Bode plots of Py-BDT and Py-Ph-BDT CMPs.

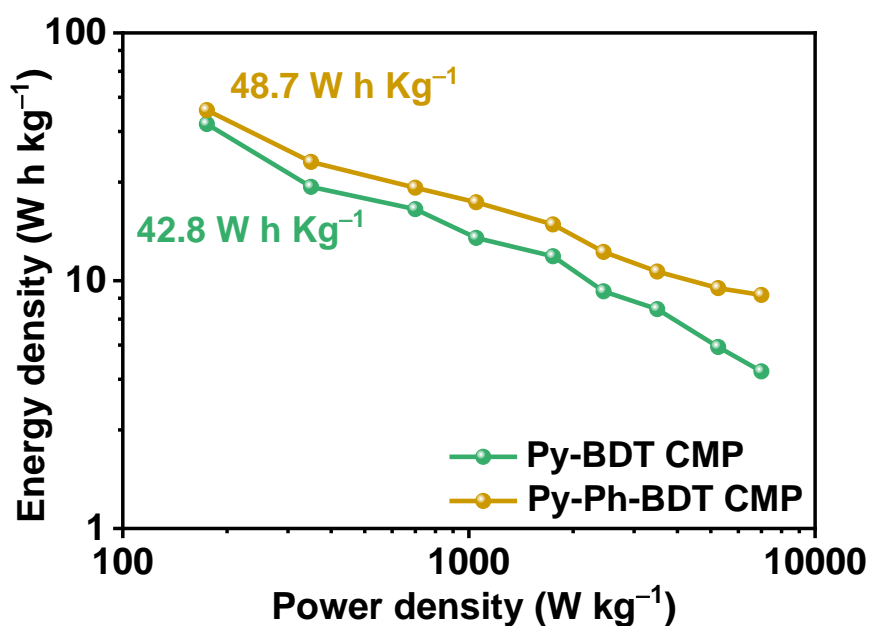


**Figure S20.** Ragone plots of energy density versus power density for the Py-BDT and Py-Ph-BDT CMPs.

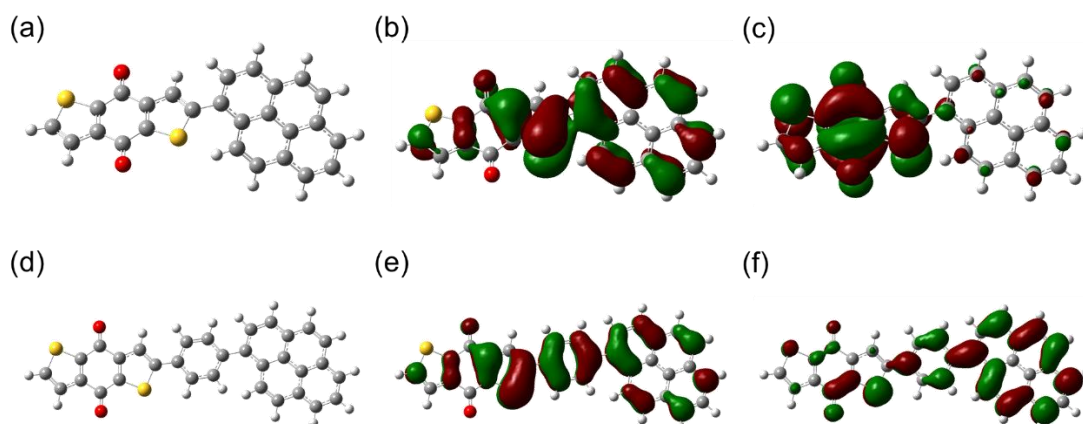


**Figure S21.** (a,d) The optimized geometry, (b,e) the HOMO distribution, and (c,f) LUMO distribution of the (a-c) Py-BDT and (d-f) Py-Ph-BDT CMPs.

### S13. Electrochemical Analysis in Two-Electrode Symmetric Supercapacitor System

The slurry prepared by mixing CMP (70 wt. %), carbon black (20 wt. %), and Nafion (10 wt. %) was coated onto a Kuraray carbon paper (0.1 mm in thickness) with an effective area of 1 cm × 1 cm and then dried at 100 °C overnight in a vacuum oven. The mass loading of active material on the current collector was 0.8 mg cm<sup>-2</sup>. The two

working electrodes was separated with filter paper and infiltrated with a potassium hydroxide (1 M) aqueous solution.

The specific capacitance was calculated from galvanostatic charge–discharge experiments using the following equation:<sup>S6</sup>

$$C_s = 2 \times (I\Delta t)/(m\Delta V) \quad (S4)$$

Where  $C_s$  (F/g) is specific capacitance of the supercapacitor,  $I$  (A) is the discharge current,  $\Delta V$  (V) is the potential window,  $\Delta t$  (s) is the discharge time, and  $m$  (g) is the mass of CMP on the one electrode.

#### **S14. Electrochemical Analysis in Two-Electrode Symmetric Supercapacitor System with organic electrolyte**

The slurry prepared by mixing CMP (70 wt. %), carbon black (20 wt. %), and Nafion (10 wt. %) was coated onto a Kuraray carbon paper (0.1 mm in thickness) with an effective area of 1 cm × 1 cm and then dried at 100 °C overnight in a vacuum oven. The mass loading of active material on the current collector was 0.8 mg cm<sup>-2</sup>. The two working electrodes was separated with Celgard 3501 separator and infiltrated with a tetrabutylammonium hexafluorophosphate (TBAPF<sub>6</sub>, 1 M) in acetonitrile.

The specific capacitance was calculated from galvanostatic charge–discharge experiments using the following equation:<sup>S6</sup>

$$C_s = 2 \times (I\Delta t)/(m\Delta V) \quad (S4)$$

Where  $C_s$  (F/g) is specific capacitance of the supercapacitor,  $I$  (A) is the discharge current,  $\Delta V$  (V) is the potential window,  $\Delta t$  (s) is the discharge time, and  $m$  (g) is the mass of CMP on the one electrode.

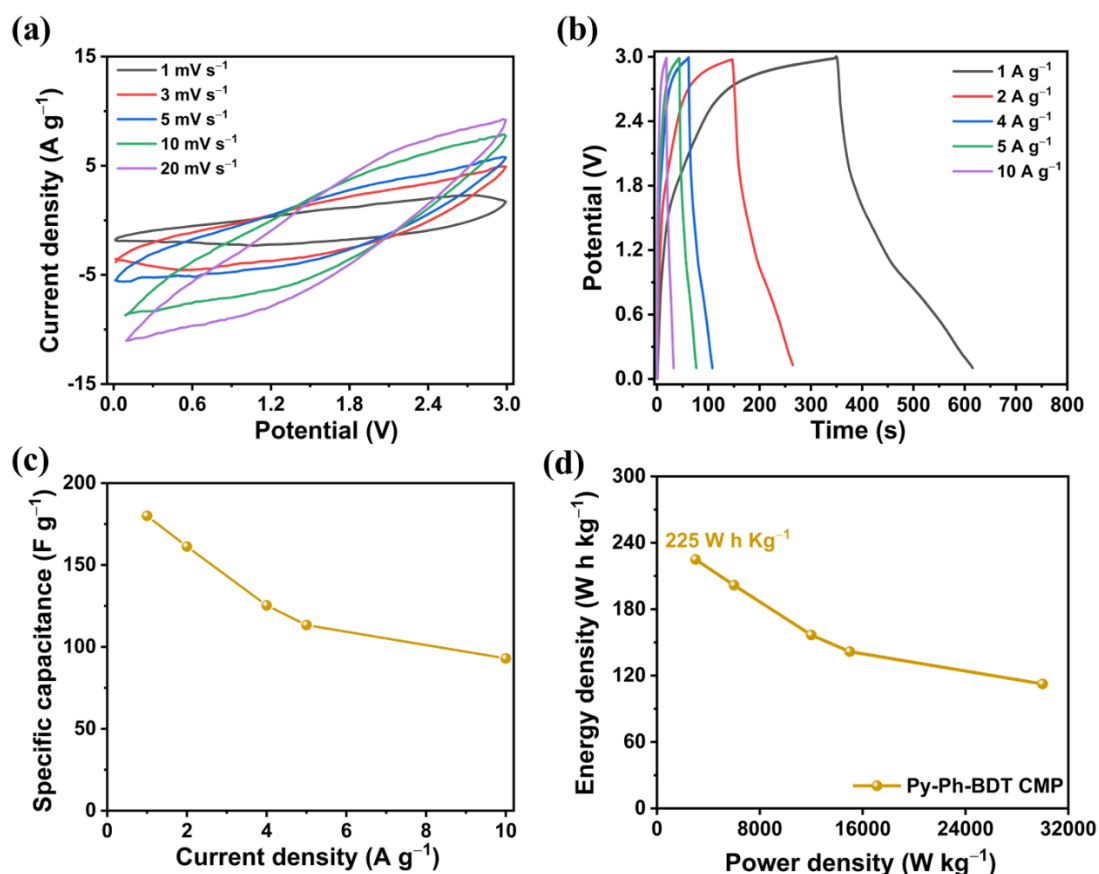


**Figure S22.** (a) CV curves of the Py-Ph-BDT CMP-tethered SC in the organic electrolyte. (b) GCD curve of the Py-Ph-BDT CMP-tethered SC in the organic electrolyte. (c) Calculated specific capacitances of Py-Ph-BDT CMP-tethered SC in the organic electrolyte. (d) Ragone plot of energy density versus power density for the Py-Ph-BDT CMP-tethered SC in the organic electrolyte.

## S15. References

- S1. P. Rios, T. S. Carter, T. J. Mooibroek, M. P. Crump, M. Lisbjerg, M. Pittelkow, N. T. Supekar, G. J. Boons and A. P. Davis, *Angew. Chem. Int. Ed.*, 2016, **55**, 3387-3392.
- S2. A. F. M. EL-Mahdy, Y. H. Hung, T. H. Mansoure, H. H. Yu, T. Chen, S. W. Kuo, *Chem. Asian J.* 2019, **14**, 1429–1435.
- S3. A. F. M. EL-Mahdy, C. Young, J. Kim, J. You, Y. Yamauchi, S. W. Kuo, *ACS Appl. Mater. Interfaces* 2019, **11**, 9343–9354.
- S4. C. R. DeBlase, K. E. Silberstein, T.–T. Truong, H. D. Abruña, W. R. Dichtel, *J. Am. Chem. Soc.*, 2013, **135**, 16821–16824.
- S5. A. Alabadi, X. Yang, Z. Dong, Z. Li, B. Tan, *J. Mater. Chem. A*, 2014, **2**, 11697–11705.
- S6. A. M. Khattak, H. Sin, Z. A. Ghazi, X. He, B. Liang, N. A. Khan, H. R. Alanagh, A. Iqbal, L. Li, Z. Tang, *J. Mater. Chem. A*. 2018, **6**, 18827–18832.